Journal of Alloys and Compounds 507 (2010) 230–235

Contents lists available at ScienceDirect

Journal of Alloys and Compounds

journal homepage: www.elsevier.com/locate/jallcom

Enhanced giant dielectric response in Al-substituted $La_{1.75}Sr_{0.25}NiO_4$ ceramics

Xiao Qiang Liu*, Shu Ya Wu, Xiang Ming Chen

Laboratory of Dielectric Materials, Department of Materials Science & Engineering, Zhejiang University, 38 Zheda Road, Hangzhou 310027, China

ARTICLE INFO

Article history:
Received 19 June 2010
Accepted 24 July 2010
Available online 4 August 2010

Keywords:
Giant dielectric response
Impedance spectrum

ABSTRACT

The structures and dielectric properties of $La_{1.75}Sr_{0.25}Ni_{1-x}Al_xO_4$ ($x = 0$, 0.3) ceramics were presented. A single tetragonal phase was found in $La_{1.75}Sr_{0.25}NiO_4$ ceramics, while minor secondary phases were presented in $La_{1.75}Sr_{0.25}Ni_{0.7}Al_{0.3}O_4$ ceramics. Giant dielectric response was found in these ceramics. The dielectric constant was enhanced while the dielectric loss was suppressed by partially substituting nickel with aluminum ions. After comparing the activation energies of dielectric relaxation and electrical resistivity, we concluded that the overlapped low frequency dielectric relaxation was attributed to grain boundaries, while the normal low-temperature relaxation was mainly attributed to the bulk factor, that was, thermally activated small polaronic hopping in $La_{1.75}Sr_{0.25}NiO_4$ ceramics. For $La_{1.75}Sr_{0.25}Ni_{0.7}Al_{0.3}O_4$ ceramics, the low-temperature dielectric relaxation was also mainly attributed to the bulk factor. The enhanced dielectric response should be benefited from the strengthened grain boundary layer capacitor effect in $La_{1.75}Sr_{0.25}Ni_{0.7}Al_{0.3}O_4$ ceramics.

1. Introduction

Materials with giant dielectric constant have been of interest since the discovery of $CaCu_3Ti_4O_{12}$ (CCTO) for their potential application in the microelectronics [1–16]. The common feature of these materials is a giant dielectric constant ($\varepsilon' > 10^4$) over a wide range of temperature, and a sharp decrease of permittivity with increasing the frequency or decreasing the temperature to a critical point without any detectable phase transition. Among these materials, the nickelates with a K_2NiF_4 structure are highlighted for their giant dielectric response up to high frequencies. This response is observed even up to gigahertz at room temperature [13], and this feature maybe allows a potential application of these materials at high frequencies. In our previous work, the giant dielectric responses up to high frequency are observed in the $Ln_{2-x}Sr_xNiO_4$ (Ln = La, Nd, Sm, and $x = 0.25$, 0.5) ceramics [8–10]. The dielectric constant increases with increasing strontium content or decreasing ionic radius of rare earth element, while the dielectric losses are nearly unaffected. The best dielectric properties are obtained in $Sm_{1.5}Sr_{0.5}NiO_4$ ceramics, that is, the dielectric constant is about 100,000 at high frequency, and the dielectric loss is only about 0.1. The valuable characteristic of this ceramics is that this giant dielectric constant is stable over a wide temperature (200–500 K) and frequency (10 kHz to 5 MHz) range. We have proved the giant dielectric response in these ceramics is attributed to the thermally activated hopping of small polarons, and the significant decrease of dielectric constant under a critical temperature is readily explained by the segregation of these polarons, which is due to the formation of stripe charge ordering under the critical temperature. However, the dielectric loss is not small enough to meet the requirement of the practical application. So, the key challenge in these materials is to suppress the dielectric loss without degrading the giant dielectric constant.

The high dielectric loss is mainly attributed to the high electrical conductivities of these materials, and the dielectric loss may be suppressed by decreasing the electrical conductivity. The electrical conductivity can be suppressed by the following two ways: (1) decrease the content of strontium since the electrical conductivity decreases with decreasing the strontium content [17] and (2) substitute Ni^{3+} by invariable trivalent ions, such as Al^{3+} ions, because the major transport carriers are the holes in t_{2g} orbits of Ni^{3+} ions in these materials [18]. In the present work, we combine the above-mentioned two ways to obtain the $La_{1.75}Sr_{0.25}Ni_{0.7}Al_{0.3}O_4$ ceramics with enhanced giant dielectric constant and suppressed dielectric loss.

2. Experimental conditions

$La_{1.75}Sr_{0.25}Ni_{1-x}Al_xO_4$ ($x = 0$, 0.3) powders were prepared by a solid-state reaction with using La_2O_3 (99.99%), NiO (99%), Al_2O_3 (99.99%) and $SrCO_3$ (99.9%) as starting materials. The weighted raw materials were mixed by ball milling with ZrO_2 media in ethanol for 24 h, and then the dried mixtures were calcined at 1200 °C for 3 h to yield desired materials. The calcined products were reground with 8 vol% of polyvinyl alcohol (PVA) binder before being pressed uniaxially into pellets. The pellets were sintered at 1425 and 1525 °C in air for 3 h to obtain desired and dense ceramics for $La_{1.75}Sr_{0.25}NiO_4$ and $La_{1.75}Sr_{0.25}Ni_{0.7}Al_{0.3}O_4$, respectively. The crystalline phases of sintered samples after crushing and grinding were identified by powder X-ray diffraction (XRD) using Cu Kα radiation (Rigaku D/max 2550 PC, Rigaku Co.,

* Corresponding author. Tel.: +86 571 87951410; fax: +86 571 87951410.
E-mail address: xqliu@zju.edu.cn (X.Q. Liu).

0925-8388/$ – see front matter © 2010 Elsevier B.V. All rights reserved.
doi:10.1016/j.jallcom.2010.07.163

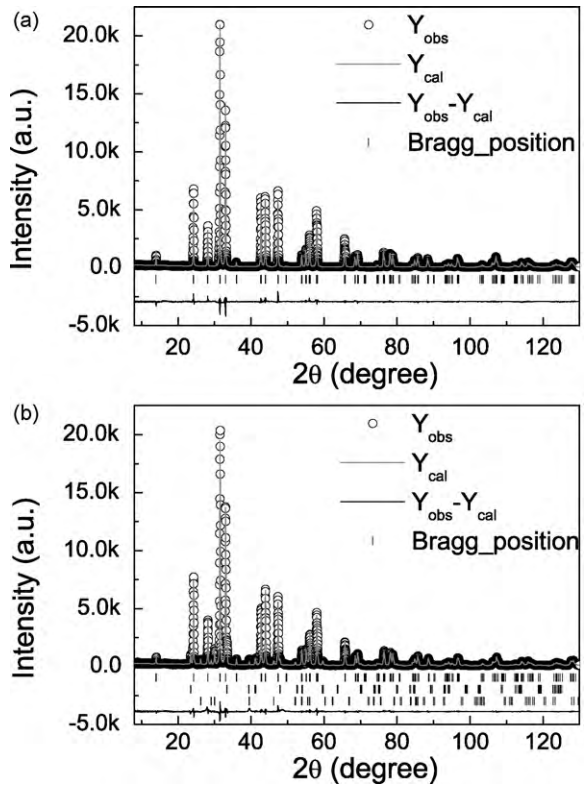

Fig. 1. Rietveld refined results of X-ray diffraction pattern for (a) $La_{1.75}Sr_{0.25}NiO_4$ and (b) $La_{1.75}Sr_{0.25}Ni_{0.7}Al_{0.3}O_4$ ceramics at room temperature. The Bragg positions of $La_{1.75}Sr_{0.25}Ni_{0.7}Al_{0.3}O_4$ ceramics are belong to $La_{1.75}Sr_{0.25}Ni_{0.7}Al_{0.3}O_4$, $LaAlO_3$ and La_2O_3 phases from top to bottom, respectively.

Tokyo, Japan). The XRD data for Rietveld refinement were collected over a 2θ range of 8–130° with a step size of 0.02° and a count of time of 1 s. The Rietveld refinement was performed using the FULLPROF package, and a pseudo-Voigt profile function with preferred orientation correction was used [19,20]. The microstructures were observed from as-sintered surfaces of these ceramics with a field emission scanning electron microscopy (S-4800, Hitachi Co., Tokyo, Japan). The backscattered electron micrographs of as-sintered surfaces of $La_{1.75}Sr_{0.25}Ni_{0.7}Al_{0.3}O_4$ ceramics were observed with a scanning electron microscopy (JSM-5610LV, JEOL, Tokyo, Japan) equipped with an Oxford Link-Isis energy-dispersive X-ray analysis system (EDS). The dielectric characteristics and ac conductivities of these ceramics were evaluated with a broadband dielectric spectrometer (Turnkey Concept 50, Novocontrol Technologies GmbH & Co. KG, Hundsangen, Germany) in a broad range of temperature (123–573 K) and frequency (1 Hz to 10 MHz) with a heating rate of 2 K/min, and the silver paste was adopted as electrodes.

3. Results and discussion

Fig. 1 shows the Rietveld refined results for XRD patterns of $La_{1.75}Sr_{0.25}Ni_{1-x}Al_xO_4$ ($x = 0$, 0.3) ceramics at room temperature.

Table 2
Fractional atomic coordinates and selected bond distances from X-ray powder diffraction data of $La_{1.75}Sr_{0.25}Ni_{1-x}Al_xO_4$ ceramics.

		$x = 0$	$x = 0.3$
La/Sr	$x = y$	0	0
	z	0.36214(5)	0.36179(5)
	B (Å^2)	0.845(12)	1.000(14)
Ni/Al	$x = y = z$	0	0
	B (Å^2)	1.329(35)	0.782(42)
O1	$x = y$	0	0
	z	0.17692(41)	0.17082(44)
	B (Å^2)	1.045(99)	1.57(12)
O2	$x = z$	0	0
	y	0.5	0.5
	B (Å^2)	1.09(11)	0.87(12)
2 × Ni–O1 (Å)		2.246(5)	2.164(5)
4 × Ni–O2 (Å)		1.919091(4)	1.918344(5)

For $La_{1.75}Sr_{0.25}NiO_4$ ceramics, a single tetragonal phase is found in the space group of $I4/mmm$. While for $La_{1.75}Sr_{0.25}Ni_{0.7}Al_{0.3}O_4$ ceramics, besides the main tetragonal $La_{1.75}Sr_{0.25}Ni_{0.7}Al_{0.3}O_4$ phase, minor impurities, $LaAlO_3$ and La_2O_3 phases, are observed in the XRD patterns. The abundances of these two secondary phases are 6.84(10) wt% and 2.04(3) wt%, respectively. Since some impurities are presented, we have tried to refine occupies of La/Sr and Ni/Al ions for sample with $x = 0.3$, but no reasonable result can be achieved. So we fix occupies of these ions as the expected ones. The experimental parameters of XRD for $La_{1.75}Sr_{0.25}Ni_{1-x}Al_xO_4$ ($x = 0$, 0.3) ceramics are shown in Table 1. The cell volume decreases with partially substituting nickel by aluminum ions, and this should be resulted from the smaller ionic radius of aluminum. The fractional atomic coordinates and selected bond distances refined from XRD data for $La_{1.75}Sr_{0.25}Ni_{1-x}Al_xO_4$ ($x = 0$, 0.3) ceramics are also shown in Table 2. The positions of La/Sr ions are nearly unchanged, while the apical oxygen (O1) of Ni–O6 octahedron moves toward nickel ion when the partial nickel is substituted by aluminum ions. Although the lengths of Ni/Al–O1 and Ni/Al–O2 bonds both decrease with increasing x, the magnitude of reduction for Ni/Al–O1 bond is larger than that of Ni/Al–O2 bond. This should be attributed to the degradation of Jahn–Teller effect [18]. Fig. 2 shows the micrographs of the as-sintered surfaces of $La_{1.75}Sr_{0.25}Ni_{1-x}Al_xO_4$ ($x = 0$, 0.3) ceramics. Dense ceramics are obtained, and the grain size increases with increasing the value of x. The distributions of grain sizes are inhomogeneous in these ceramics. We have tried to use the backscattered electron mode to identify impurities in ceramics with $x = 0.3$ since two minor secondary phases are identified by XRD pattern. Unfortunately, no contrast is detected in micrographs, and EDS results show the chemical components at different grains are nearly unchanged. This may be resulted from the following two rea-

Table 1
Experimental parameters for X-ray powder diffraction of $La_{1.75}Sr_{0.25}Ni_{1-x}Al_xO_4$ ceramics.

	$x = 0$	$x = 0.3$
Unit cell (space group $I4/mmm$)	$a = b = 3.83818(6)$ Å $c = 12.69572(21)$ Å	$a = b = 3.83669(7)$ Å $c = 12.67155(26)$ Å
Cell volume	187.029(5) Å^3	186.527(6) Å^3
Number of reflections	142	145
Number of refined parameters	24	33
Half width parameters	$U = 0.0463(25)$, $V = -0.0165(27)$, $W = 0.02307(68)$, $X = 0.00585(26)$	$U = 0.0673(41)$, $V = -0.0201(40)$, $W = 0.02739(96)$, $X = 0.00535(31)$
Peak shape (Pseudo-Voigt), η	0.4194(126)	0.4522(144)
Zero-point, 2θ (°)	−0.0238(11)	−0.0252(14)
Preferred orientation [1 1 0]	1.0323(30)	1.0397(32)
Asymmetry parameter	$P_1 = 0.0661(47)$, $P_2 = 0.0319(10)$	$P_1 = 0.0387(51)$, $P_2 = 0.0328(11)$
Reliability factors	$R_p = 6.00$, $R_{wp} = 8.01$, $\chi^2 = 2.29$	$R_p = 6.01$, $R_{wp} = 9.34$, $\chi^2 = 3.30$
Abundances of impurities	–	$LaAlO_3$: 6.84(10) wt%, La_2O_3: 2.04(3) wt%

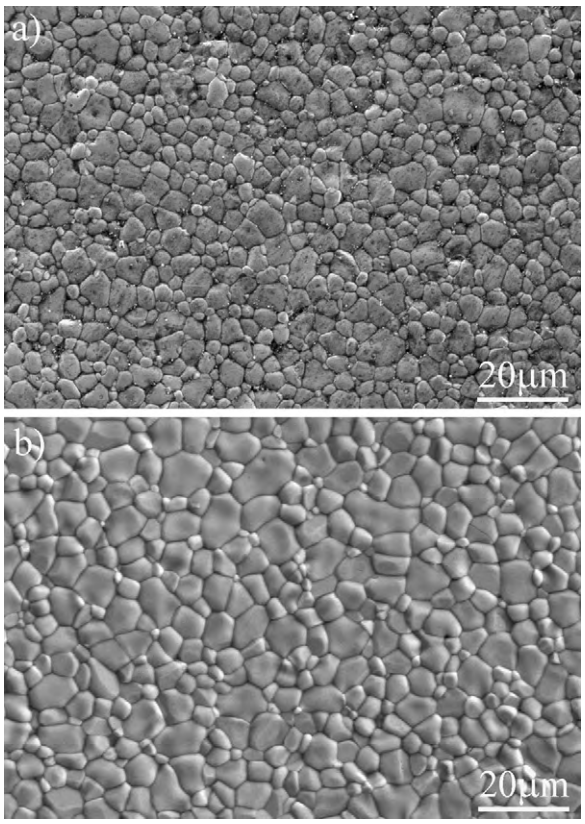

Fig. 2. SEM micrographs of as-sintered surfaces of $La_{1.75}Sr_{0.25}Ni_{1-x}Al_xO_4$ ceramics (a) $x = 0$ and (b) $x = 0.3$.

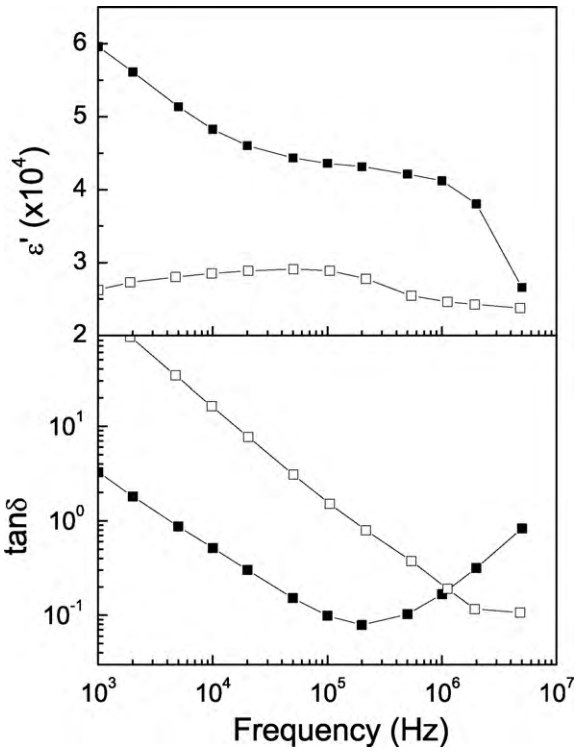

Fig. 3. Frequency dependence of dielectric properties of $La_{1.75}Sr_{0.25}NiO_4$ (□) and $La_{1.75}Sr_{0.25}Ni_{0.7}Al_{0.3}O_4$ (■) ceramics at room temperature.

sons: (1) there is small difference in chemical components between the secondary and main phase, and (2) the minor secondary phase locates at grain boundaries instead of the grain interiors. For $LaAlO_3$ phase, nickel and strontium can incorporate into the aluminum and lanthanum sites, respectively, and so, the chemical components maybe are slightly different from those of the main phase. As a result, no detectable contrast is found in the backscattered electron micrographs. For La_2O_3 secondary phase, the possibility of replacement of elements as in $LaAlO_3$ phase is small, so we infer this secondary phase should locate at the grain boundaries. These insulating secondary phases will enhance the electrical resistivity of the grain boundaries for the present ceramics.

The dielectric properties of $La_{1.75}Sr_{0.25}Ni_{1-x}Al_xO_4$ ($x = 0$, 0.3) ceramics at room temperature are shown in Fig. 3. The dielectric constant is enhanced by partially substituting nickel with

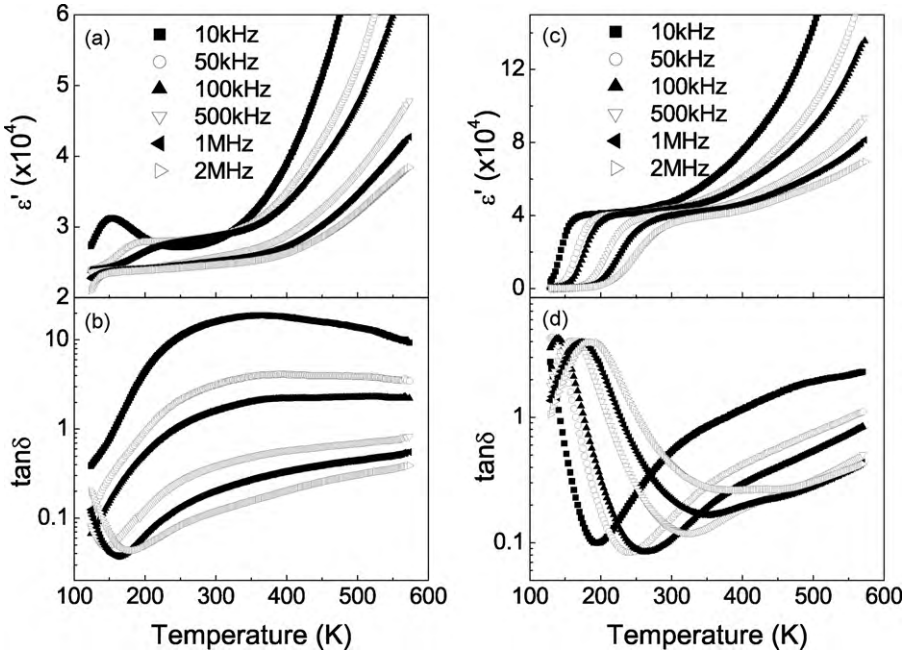

Fig. 4. Temperature dependence of dielectric constant and loss for $La_{1.75}Sr_{0.25}Ni_{1-x}Al_xO_4$ ceramics at various frequencies: (a) and (b) for $x = 0$, and (c) and (d) for $x = 0.3$.

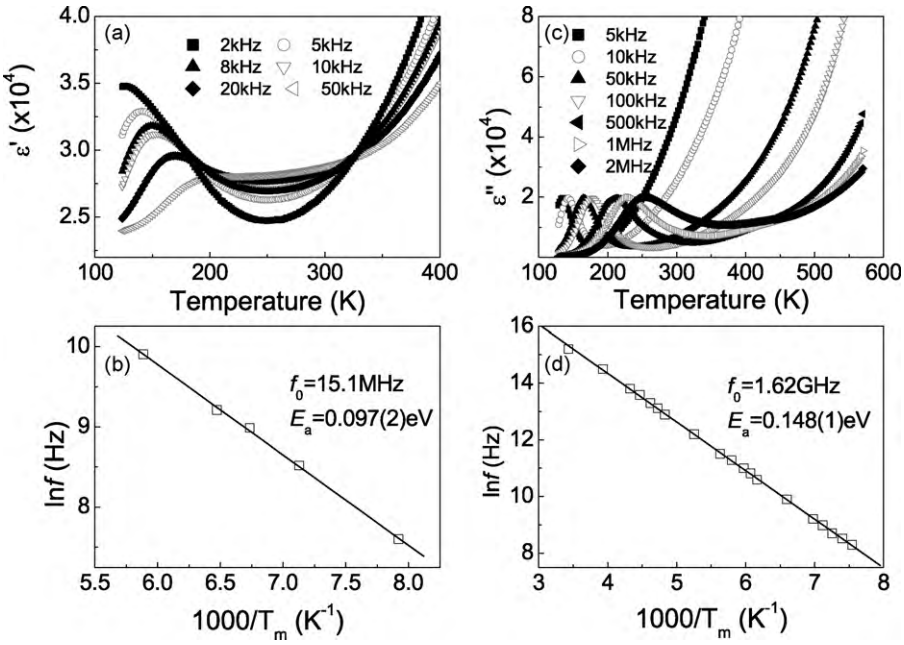

Fig. 5. Temperature dependence of permittivity for $La_{1.75}Sr_{0.25}Ni_{1-x}Al_xO_4$ ceramics at various frequencies, and frequency dependence of the peak temperature of permittivity for low-temperature dielectric relaxation in ceramics: (a) and (b) for $x = 0$, and (c) and (d) for $x = 0.3$. The squares are the experimental data and the line is the Arrhenius fitting.

aluminum ions, while the dielectric loss is suppressed at lower frequencies. At the frequency of 1 MHz, the dielectric constants are about 25,000 and 45,000 for ceramics with $x = 0$ and 0.3, respectively, and the dielectric losses are both about 0.2. Fig. 4 shows the temperature dependence of dielectric properties of $La_{1.75}Sr_{0.25}Ni_{1-x}Al_xO_4$ ($x = 0$, 0.3) ceramics. Multiple dielectric relaxations are found in these ceramics. The low-temperature dielectric relaxation is the onset of giant dielectric response step. The dielectric constant significantly increases when the temperature is larger than a critical temperature, and the critical temperature increases with increasing frequency. Noted this dielectric relaxation is occurred around the charge-ordering temperature for ceramics with $x = 0$, and this indicates the correlation between the dielectric relaxation and charge order–disorder transition [16]. At temperatures above 400 K, the dielectric constant sharply increases with increasing temperature, and the phenomena are more obvious at lower frequencies. An overlapped dielectric relaxation around 150 K is observed at low frequency in ceramics with $x = 0$, and this low frequency dielectric relaxation is more clearly shown in Fig. 5a. This dielectric relaxation is only existed at low frequencies and it will disappear at frequencies above 50 kHz. After plotting peak temperatures as functions of frequencies (as shown in Fig. 5b), the Arrhenius fitting is carried out on these points, and an activation energy of 0.097 ± 0.002 eV is obtained by this fitting. A very small f_0 value of 15.1 MHz is also obtained, and this further confirms the overlapped dielectric relaxation is only existed at low frequency. For ceramics with $x = 0.3$, the temperature dependence of imaginary dielectric constant is shown in Fig. 5c. Again the Arrhenius fitting is carried out on the curve of frequency dependence of peak temperature, and an activation energy of 0.148 ± 0.001 eV with a much larger f_0 value of 1.62 GHz is obtained. To get a deep insight into this dielectric relaxation in the ceramics with $x = 0.3$, the frequency dependence of dielectric constants at various temperatures is plotted and shown in Fig. 6a. The modified Debye equation is employed to fit the curve [21],

$$\varepsilon^* = \varepsilon' - i\varepsilon'' = \varepsilon_\infty + \frac{(\varepsilon_0 - \varepsilon_\infty)}{[1 + (i\varpi\tau)^{1-\alpha}]} \quad (1)$$

where ε_0 is static dielectric constant, ε_∞ is the dielectric constant at very high frequencies, ω is the angular frequency, τ is the mean relaxation time and α represents the degree of distribution of relaxation time τ. By fitting the experimental data, we obtain the mean relaxation times τ at different temperatures, and plot τ as a function

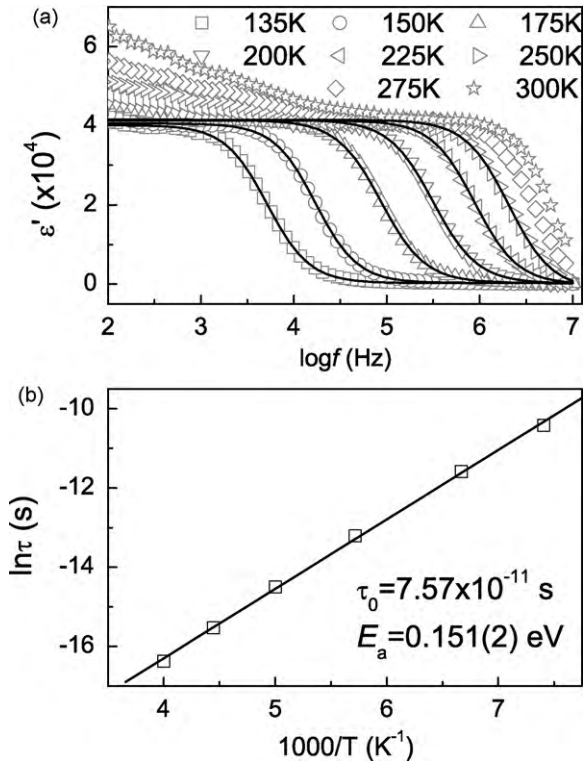

Fig. 6. (a) Frequency dependence of dielectric constant for $La_{1.75}Sr_{0.25}Ni_{0.7}Al_{0.3}O_4$ ceramics at various temperatures. The solid line is the modified Debye fitting. (b) Temperature dependence of dielectric relaxation times for low-temperature dielectric relaxation in the ceramics. The squares are the experimental data and the line is the Arrhenius fitting.

of reciprocal temperature as shown in Fig. 6b. The variation of relaxation times with temperatures obeys thermally activated Arrhenius law, and an activation energy of 0.151 ± 0.002 eV is resulted, which is consistent with that obtained from the curve of temperature dependence of imaginary dielectric constant.

To find out the origin of giant dielectric responses in the present ceramics, the impedance spectra are used to determine contributions from bulk (grain interiors) and grain boundaries [22,23]. For a typical electroceramics, the equivalent circuit consisting of two parallel *RC* elements connected in series with one *RC* element, $R_{gb}C_{gb}$, representing grain boundary regions and the other one, R_bC_b, representing the bulk, is usually used to fit the experiment data. As pointed by Sinclair [22], the advantage of combined imaginary electric modulus (M'') and imaginary impedance (Z'') plots is a rapid assessment of the values of R and C can be made from a visual inspection of such plot. So in the present work, we use the combined M'' and Z'' plots, and results are shown in Fig. 7 for ceramics with $x = 0.3$. There is only one peak at the Z'' plot when the temperature is higher than 200 K, which demonstrates the difference between values of R_{gb} and R_b is very large. There are two peaks in the M'' plot, which denotes the difference between values of C_{gb} and C_b is small. Meanwhile, we use the above-mentioned equivalent circuit to fit the experiment data, and resulted parameters are shown in Table 3. The values of R and C confirm the previous assessments on the combined M'' and Z'' plots. The resistivity decreases with increasing temperature, while the C_{gb} value varies slightly in the considered temperature range. The value of C_b increases smoothly first and then grows sharply when the temperature is larger than 275 K. This temperature is consistent with that of the onset of giant dielectric step. The same phenomenon is also found in other $Ln_{2-x}Sr_xNiO_4$ ceramics, which indicates the same dielectric relaxation mechanism should exist in the present ceramics, that is, the thermally activated small polaronic hopping. For ceramics with $x = 0$, the above-mentioned equivalent circuit cannot fit the experimental data well. So the least-mean-square analyses are employed to determine resistivities of grain boundaries and bulk [24], and results are shown as dots in Fig. 8a. The difference between values of R_{gb} and R_b for ceramic with $x = 0.3$ is larger than that for $x = 0$, which indicates the grain boundary layer capacitor (GBLC) effect plays a more important role in ceramics with $x = 0.3$ than that for $x = 0$ (Ref. [25]). In order to clearly illustrate the correlation between dielectric relaxation and small polaronic hopping conduction, the adiabatic small polaronic conductive mechanism is used to fit resistivities obtained from impedance spectra [8,9,17], and results are shown as the solid lines in Fig. 8. The variations of resistivities of these ceramics with temperature obey small polaronic hopping conductive mechanism in the considered temperature range. For ceramics with $x = 0$, an activation energy of grain boundaries is 0.088 ± 0.003 eV, and that of bulk is 0.037 ± 0.002 eV. The activation energy of grain boundaries is similar to that of the overlapped low frequency dielectric relaxation at low temperature. Combining with the resulted small value of f_0, we conclude the low frequency dielectric relaxation should be attributed to grain boundaries effects, such as Maxwell–Wagner effect. The activation energy of bulk is very small, and this value is almost same as that of $La_{1.15}Gd_{0.85}CuO_4$ phase at the low temperature (0.034 eV) [26], which is interpreted as the dipole polarization associated with 3D hopping motion of local charge centers. This also may be the origin of giant dielectric response in the present ceramics. For ceramics with $x = 0.3$, the activation energy of grain boundaries is 0.131 ± 0.001 eV, while that of bulk is 0.162 ± 0.002 eV. The activation energy of bulk is similar to that of low-temperature dielectric relaxation. From these results, we confirm the giant dielectric response is mainly attributed to the thermally activated small polaronic hopping.

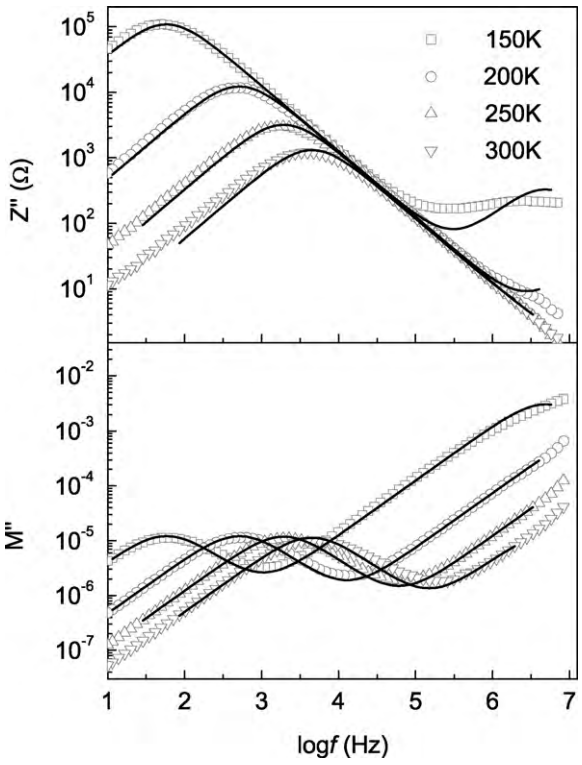

Fig. 7. Variations of impedance Z'' and modulus M'' with frequency at different temperatures for $La_{1.75}Sr_{0.25}Ni_{0.7}Al_{0.3}O_4$ ceramics. The solid lines are fitted by the equivalent circuit as shown as the insert.

Now we return to discuss the discrepancy of dielectric properties for the $La_{1.75}Sr_{0.25}NiO_4$ and $La_{1.75}Sr_{0.25}Ni_{0.7}Al_{0.3}O_4$ ceramics. The dielectric constant of $La_{1.75}Sr_{0.25}NiO_4$ ceramics is about 25,000, which is only about one third of that of $La_{1.5}Sr_{0.5}NiO_4$ ceramics [8]. As shown in the previous chapter, the giant dielectric response in these ceramics is attributed to the thermally activated small polaronic hopping, and so the dielectric constant should be direct proportional to the concentration of small polarons. The concentration of small polarons decreases with decreasing strontium content, and the dielectric constant degrades as a result. However, the dielectric constant increases with increasing the x value, and this

Table 3
Summary of the electrical parameters corresponding to the equivalent circuit model used in the fitting of the experimental data at different temperatures as shown in Fig. 7.

Temperature (K)	R_{gb} (Ω)	C_{gb} (nF)	R_b (Ω)	C_b (nF)
135	540,680 ± 29,472	12.8 ± 0.3	2101 ± 49	0.038 ± 0.002
150	220,880 ± 4564	12.6 ± 0.2	676 ± 9	0.067 ± 0.002
175	64,003 ± 630	12.59 ± 0.09	134 ± 1	0.084 ± 0.003
200	24,557 ± 123	12.67 ± 0.05	38.7 ± 0.2	0.18 ± 0.01
225	11,674 ± 51	12.77 ± 0.05	14.2 ± 0.1	0.23 ± 0.04
250	6408 ± 29	12.92 ± 0.06	6.42 ± 0.09	0.61 ± 0.19
275	3959 ± 21	13.17 ± 0.07	3.6 ± 0.1	5.1 ± 0.2
300	2663 ± 17	13.5 ± 0.1	2.4 ± 0.2	12 ± 3
325	1894 ± 15	14.0 ± 0.1	1.8 ± 0.1	15 ± 4

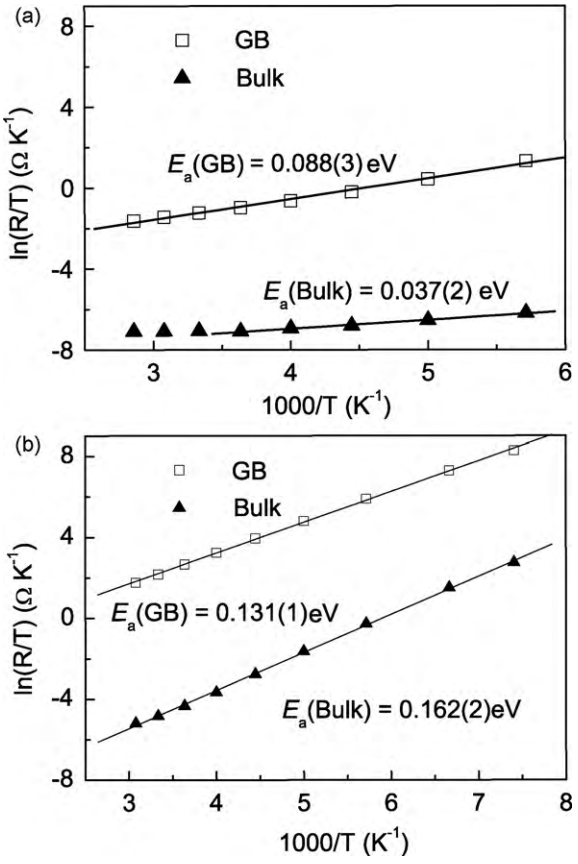

Fig. 8. Thermally activated small polaronic hopping fitting of the electrical resistances obtained from the impedance spectra of $La_{1.75}Sr_{0.25}Ni_{1-x}Al_xO_4$ ceramics: (a) $x = 0$ and (b) $x = 0.3$.

cannot be explained by the concentration change of small polarons since they should decrease with increasing aluminum content. Another factor should affect dielectric properties of the present ceramics. As shown in the previous chapter, the GBLC effect will play a more important role in the present ceramics than the parent compound, and so the enhanced dielectric response should be resulted from the strengthened GBLC effect. On the other hand, the decease of dielectric loss by partially substituting nickel with aluminum should be resulted from the decrease of electrical conductivity as shown in Fig. 8.

4. Conclusion

Dense $La_{1.75}Sr_{0.25}Ni_{1-x}Al_xO_4$ ($x = 0$, 0.3) ceramics are prepared by solid-state sintering. A single tetragonal phase is obtained for ceramics with $x = 0$, while two minor secondary phases accompanying with the main tetragonal phase are found in ceramics with $x = 0.3$. The dielectric constant increases from 25,000 to 45,000 when x value increases from 0 to 0.3, while the dielectric losses are both about 0.2 at frequency of 1 MHz and room temperature. There are multiple dielectric relaxations in the present ceramics, and the low-temperature relaxation is the onset of giant dielectric constant step. An overlapped low frequency dielectric relaxation is found at low temperature for ceramics with $x = 0$. From the close correlation between the activation energy of dielectric relaxation and electrical conductivity, the overlapped low frequency dielectric relaxation should be due to the grain boundaries effects, such as, Maxwell–Wagner effect, while the normal low-temperature relaxation should be mainly attributed to the thermally activated small polaronic hopping in these two ceramics. The enhanced dielectric response should be benefited from the strengthened grain boundary layer capacitor effect in $La_{1.75}Sr_{0.25}Ni_{0.7}Al_{0.3}O_4$ ceramics.

Acknowledgments

This work was supported by National Science Foundation of China under Grant Nos. 50702049 and 50832005.

References

[1] M.A. Subramanian, D. Li, N. Duan, B.A. Reisner, A.W. Sleigh, J. Solid State Chem. 151 (2000) 323.
[2] C.C. Homes, T. Vogt, S.M. Shapiro, S. Wakimoto, A.P. Ramirez, Science 293 (2001) 673.
[3] L. Ni, X.M. Chen, J. Am. Ceram. Soc. 93 (2010) 184.
[4] J. Wu, C.-W. Nan, Y. Lin, Y. Deng, Phys. Rev. Lett. 89 (2002) 217601.
[5] Y. Lin, J. Wang, L. Jiang, Y. Chen, C.-W. Nan, Appl. Phys. Lett. 85 (2004) 5664.
[6] I.P. Raevski, S.A. Prosandeev, A.S. Bogatin, M.A. Malitskaya, L. Jastrabik, J. Appl. Phys. 93 (2003) 4130.
[7] Z. Wang, X.M. Chen, L. Ni, X.Q. Liu, Appl. Phys. Lett. 90 (2007) 022904.
[8] X.Q. Liu, S.Y. Wu, X.M. Chen, H.Y. Zhu, J. Appl. Phys. 104 (2008) 054114.
[9] X.Q. Liu, Y.J. Wu, X.M. Chen, H.Y. Zhu, J. Appl. Phys. 105 (2009) 054104.
[10] X.Q. Liu, C.L. Song, X.M. Chen, H.Y. Zhu, Ferroelectrics 388 (2009) 161.
[11] C.L. Song, Y.J. Wu, X.Q. Liu, X.M. Chen, J. Alloys Compd. 490 (2010) 605.
[12] T. Park, Z. Nussinov, K.R.A. Hazzard, V.A. Sidorov, A.V. Balatsky, J.L. Sarrao, S.W. Cheong, M.F. Hundley, J.S. Lee, Q.X. Jia, J.D. Thompson, Phys. Rev. Lett. 94 (2005) 017002.
[13] S. Krohns, P. Lunkenheimer, Ch. Kant, A.V. Pronin, H.B. Brom, A.A. Nugroho, M. Diantoro, A. Loidl, Appl. Phys. Lett. 94 (2009) 122903.
[14] M. Filippi, B. Kundys, S. Agrestini, W. Prellier, H. Oyanagi, N.L. Saini, J. Appl. Phys. 106 (2009) 104116.
[15] Y. Hou, Y.P. Yao, G.Q. Zhang, Q.X. Yu, X.G. Li, J. Am. Ceram. Soc. 92 (2009) 1366.
[16] P. Lunkenheimer, S. Krohns, S. Riegg, S.G. Ebbinghaus, A. Reller, A. Loidl, Eur. Phys. J. Special Topics 180 (2010) 61.
[17] G. Wu, J.J. Neumeier, Phys. Rev. B 67 (2003) 125116.
[18] T. Hotta, Rep. Prog. Phys. 69 (2006) 2061.
[19] R.A. Young, The Rietveld Method, Oxford Science Publications, New York, 1993.
[20] J. Rodriguez-Carvajal, Commission on Powder Diffraction (IUCr) Newsletters, vol. 26, 2001, p. 12.
[21] K.S. Cole, R.H. Cole, J. Chem. Phys. 9 (1941) 341.
[22] D.C. Sinclair, A.R. West, J. Appl. Phys. 66 (1989) 3850.
[23] R. Gerhardt, J. Phys. Chem. Solids 55 (1994) 1491.
[24] E. Iguchi, H. Nakatsugawa, K. Futakuchi, J. Solid State Chem. 139 (1998) 176.
[25] T.B. Adams, D.C. Sinclair, A.R. West, J. Am. Ceram. Soc. 89 (2006) 3129.
[26] J.B. Shi, Physica C 305 (1998) 35.